

Autonomous Surgical Robot using Visual Servoing in the Extended Image Plane^{*}

C. Pérez, R. Morales, N. García-Aracil, J.M. Azorín, J.M. Sabater^{*}
E. Cervera^{**}

^{*} *Virtual Reality and Robotics Lab., Miguel Hernández University,
03202 Elx, Alicante, Spain; e-mail: nicolas.garcia@umh.es).*

^{**} *Robotic Intelligence Lab. Jaume I University, 12071 Castellón,
Spain*

Abstract: This paper deals with the visibility problems occurring during the execution of a visual servoing task by a robotic scrub nurse. To deliver the instrument to the surgeon and to retrieve that instrument when the surgeon is finished using it, are the vision guide tasks to be performed by the robot. One of the main problems of a vision guide robotic scrub nurse is the lose of some image features during the control process. This problem can be produced by a temporal occlusion or an out-coming of one or more image features. When this problem appears, the common solution is simply stopped the visual servoing control task and started an initialization process. The solution proposed by the authors is to extend the image plane and compute the image features projected on it by a new prediction algorithm based on a sugeno type fuzzy system since computer vision methods can not be used because of the features are not visible. Experimental results demonstrate the improvements that can be obtained in the performance of the vision-based control task when the visual servoing in the extended image plane is used.

1. INTRODUCTION

With the rapid changes in medical robotics it is clear that the place where surgical procedures will be performed must change. New technologies require a new approach. Until now, the operating room has been an empty space filled with supplies, furniture, anesthesia machines, lights, etc and the surgical team (surgeon, assistant surgeon, scrub and circulating nurse, anesthesiologist, etc). During the surgery, the scrub nurse assists the surgeon and the physician assistant in the operating room (OR) by passing instruments, suctioning blood and maintaining the sterile field. Michael Treat of Columbia University has designed a robotic scrub nurse with responds appropriately to verbal requests, handing the needed instrument to the surgeon and picking up and returning the used instrument to the surgical tray [1]. The system already has performed in an actual surgery at the NewYork-Presbyterian Hospital. This robotic scrub nurse developed by Robotic Surgical Tech Inc. retrieves the instrument from a "transfer zone" or "drop zone" and not from the surgeon's hand. On the other hand, the robotic system proposed by us retrieves them from the surgeon's hand by visual servoing techniques. All this systems controlled by visual servoing have a common drawback related with the robustness issue and in short with the problem of visibility in image features.

In the recent past, the robustness issue has been widely investigated: integration of multiple visual cues to achieve robustness [7, 8]; visual control law that is robust to a

general class of image processing errors [10, 11]; different approaches that constraint camera movements [12, 13, 14, 15, 16] or use the zoom [17] or move the camera backwards along its optical axis [18] to keep all points in the camera field of view during the control task .

In this paper, the problem of visibility in image features during 2D visual control task execution is presented. Most of the solutions in the literature to address this problem are based on keeping all the features in the field of view during the whole control task as it was commented before.

Contrary to these solutions, we proposed the novel concept of allowing changes of visibility in image features during the control task presented in [19, 20] for the first time. They key idea of this concept consists on allowing some features to appear in or disappear from the image through its border. In this paper, this idea is extended to the whole image space.

In [27], we described the continuity problems of the control law due to the changes of visibility in image features during a visual servoing task and also a solution to this problem when features appear/disappear through the border of the image was proposed. This solution is based on weighting image features depending on the position of them in the image plane Φ_{uv} . The weights are used in order to anticipate in some way the possible discontinuities produced in the control law by the temporary disappearance of image features through the border. Due to the definition of weight function, the image plane can be divided in two zones: Zone 1 where the weights are greater than 0 and Zone 2 where the weights are equal to 0. Between this two zones, there is a smooth transition between 1 near the center of the image and 0 in the border of Zone 1. In this

^{*} This work was supported in part by the by the Spanish Government (Research Project: High dependability in teleoperation and visual servoing for cooperative robotic tasks in medical and surgical applications ref:DPI2005-08203-C02-01/02).

case, the visual servoing task uses in the control law only the information of image features inside Zone 1 since the weight computed for the features in Zone 2 is equal to 0. In some way, we are using a reduce image plane and that reduction of image space depends on the weight function parameters used (Fig. 1).

The proposed idea is to extend the image plane instead of reducing it (Fig. 1). In this case, the image features projected on the extended image plane can not be extracted by computer vision methods because they are not visible. We evaluate two solutions to compute the position of the features in the extended image plane: the first one is to estimate their position by prediction algorithms (one of them developed by us) and the other one is to know a model of the environment and compute the pose of the object and project these features on the extend image plane assuming an acceptable camera calibration.

In this paper, visual servoing in the extended image plane using a new prediction algorithm based on a sugeno type fuzzy system is presented. In section 2, a short description of vision-based control in the extended image plane is presented. Then, the computing of the image features based on a *fuzzy* filter is described on section 3. Finally, the experimental results to show the performance of the visual servoing in the extended image plane is presented in section 4.

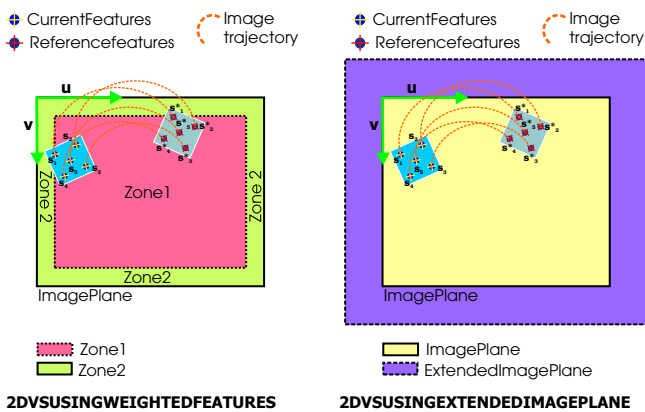


Fig. 1. 2D Visual servoing using weighted features and extended image plane

2. VISION-BASED CONTROL IN THE EXTENDED IMAGE PLANE

Consider a standard vision-based positioning task. The goal is to bring the robot end-effector back to a reference position (ξ^*) with an eye-in-hand camera. This means that a feature vector $s(\xi)$, which contains the information of the current image, has to converge to a reference feature vector $s^*(\xi^*)$. We use the task function approach [4] which consists in minimizing an error vector e :

$$e = C(s - s^*) \quad (1)$$

where C is a matrix which has to be selected such that $C L(s; Z) > 0$ in order to ensure the global stability of the control law. The optimal choice is to consider C as the pseudo-inverse $L^+(s; Z)$ of the interaction matrix. The matrix C thus depends on the depth Z of each target point used in visual servoing. In order to avoid the estimation

of Z at each iteration of the control law, one can choose C as a constant matrix equal to $L^+(s^*; Z^*)$, the pseudo-inverse of the interaction matrix computed for $s = s^*$ and $Z = Z^*$, where Z^* is an approximate value of Z at the desired camera position. In this simple case, the condition for convergence is satisfied only in the neighborhood of the desired position, which means that the convergence may not be ensured if the initial camera position is too far away from the desired one and the performed trajectory in the image space is unpredictable and some visual features may get out of the camera field of view during the control task [28] (Fig. 1).

A local exponential decrease of the task function can be imposed by choosing a proportional control law $v = -\lambda e$ where v is the velocity of the camera and λ is a positive scalar factor which tunes the speed of convergence.

$$v = -\lambda e \quad \text{where } e = \hat{L}^+(s - s^*) \quad (2)$$

On the other hand, it is well-known that visual servoing systems fail if the image features go outside the image plane during the control task (Fig. 2). We proposed in [19, 20], the first approach which allows temporary disappearance of image features during the control task. In this paper, we propose a new way of dealing with the temporary disappearance based on computing the position of the features in the extended image plane using a new filter designed by us (Fig. 3).

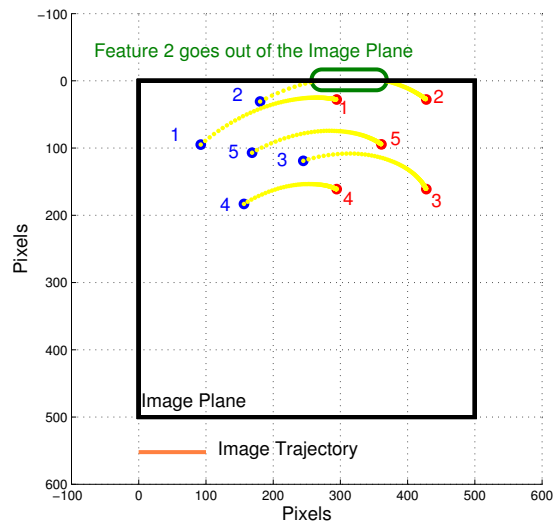


Fig. 2. 2D Visual servoing using weighted features and extended image plane

3. COMPUTING THE IMAGE FEATURES IN THE EXTENDED IMAGE PLANE

One of the main problems of visual servoing is the lose of some image features during the control process. This problem can be produced by a temporal occlusion or an out-coming of one or more image features. When this problem appears, several solutions can be used like: extract these features from s , weighted image features or simply stop the visual servoing control [19, 20, 6, 28]. As we present in Section 1, we use a filter to predict the position / trajectory of a feature \hat{s} in the extended image plane when

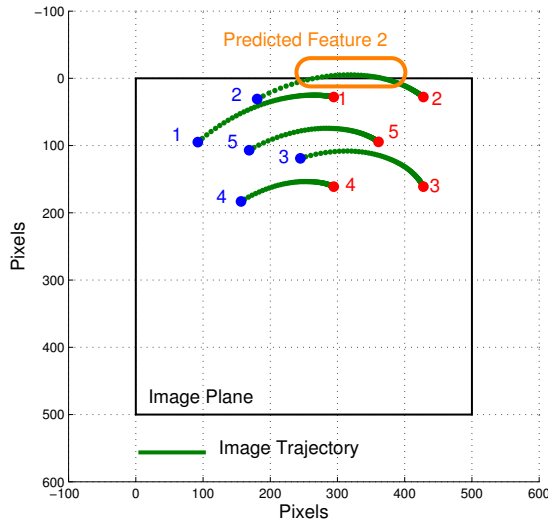


Fig. 3. 2D Visual servoing using weighted features and extended image plane

it is out of the camera FOV. The task function approach [4] which consists in minimizing an error vector \mathbf{e} is used.

$$\mathbf{e} = \mathbf{C}(\hat{\mathbf{s}} - \mathbf{s}^*) \quad \text{where } \hat{\mathbf{s}} = \mathbf{s} + \Delta \mathbf{s} \quad (3)$$

where $\Delta \mathbf{s}$ is equal to zero if the feature can be computed by computer vision techniques $\hat{\mathbf{s}} = \mathbf{s}$ and equal to the error produced by the computation of \mathbf{s} by the prediction algorithm developed. A local exponential decrease of the task function can be imposed by choosing a proportional control law $\mathbf{v} = -\lambda \mathbf{e}$ where \mathbf{v} is the velocity of the camera and λ is a positive scalar factor which tunes the speed of convergence.

$$\mathbf{v} = -\lambda \hat{\mathbf{L}}^+(\hat{\mathbf{s}} - \mathbf{s}^*) = -\lambda \hat{\mathbf{L}}^+(\mathbf{s} - \mathbf{s}^*) - \lambda \hat{\mathbf{L}}^+ \Delta \mathbf{s} \quad (4)$$

where $-\lambda \hat{\mathbf{L}}^+ \Delta \mathbf{s}$ is the perturbation due to the estimation error.

In this paper, we present a new fuzzy filter to compute the feature position in the extended image plane using the prediction of its image trajectory. This filter is based on existing filters that improves the prediction made by anyone of them. This new filter use the parameter optimization of a *Sugeno* type fuzzy system and it can be referred as: *Fuzzy FILTER*. The robustness and feasibility of the proposed algorithm is validated by a great number of experiments.

The main advantage of the proposed filter with respect to others is that adapting time is less than others and it is useful because we can lose the image feature in any moment (see Fig. 6 to see the adapting time).

3.1 Sugeno-type fuzzy interface

The most common fuzzy inference process used is known as Mamdani's fuzzy inference method. For this work, we have used the so-called *Sugeno*, or *Takagi-Sugeno-Kang (TSK)*, method of fuzzy inference. Introduced in 1985 [29], it is similar to the Mamdani method in many aspects. The first two parts of the fuzzy inference process, fuzzifying the inputs (see Figure 5) and applying the fuzzy operator, are exactly the same. The main difference between Mamdani and *Sugeno* is that the *Sugeno* output

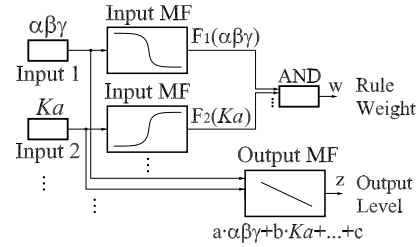


Fig. 4. *Sugeno* operation diagram

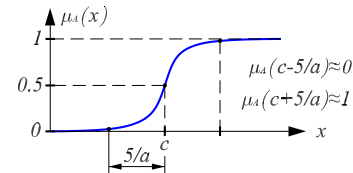


Fig. 5. Sigmoid membership function (input)

membership functions are either linear or constant (see Figure 4).

A typical rule in a *Sugeno* fuzzy model has the form: If Input 1 IS x and Input 2 IS y and ..., then Output is $z = ax + by + c$.

For a zero-order *Sugeno* model, the output level z is a constant.

The output level z_i of each rule is weighted by the firing strength w_i of the rule. For example, for an AND rule with Input 1 = $\alpha\beta\gamma$, Input 2 = Ka , ... the firing strength is:

$$w_i = \text{AndMethod}(F_1(\alpha\beta\gamma), F_2(Ka), \dots)$$

where $F_{1,2,\dots}(\cdot)$ are the membership functions for Inputs 1, 2, ...

The final output of the system is the weighted average of all rule outputs, computed as:

$$\text{FinalOutput} = \frac{\sum_{i=1}^N (w_i z_i)}{\sum_{i=1}^N (w_i)} \quad (5)$$

A *Sugeno* rule operates as shown in Figure 4 and for inputs, we have used the *sigmoide* function as we can see in Figure 5 and in expression 6.

$$\text{sigmoide}(x, a, c) = \frac{1}{1 + e^{-a(x-c)}} \quad (6)$$

3.2 The fuzzy filter

We have developed a new filter that has not a constant model of object movement, the model is estimated depending of the speed, acceleration and jerk using these simple expressions:

$$v_k = \frac{x_{k-1} - x_k}{T}; a_k = \frac{v_{k-1} - v_k}{T}; J_k = \frac{a_{k-1} - a_k}{T}$$

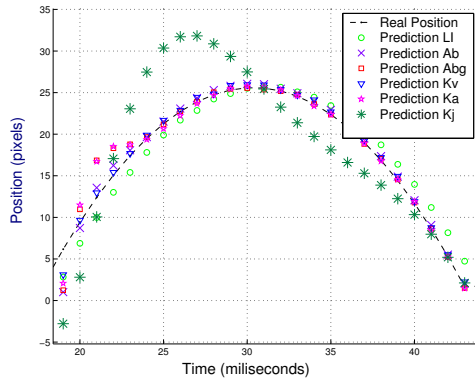


Fig. 6. 1 dof feature trajectory

Depending of these values, we apply an specific combination of filters. Filters considered are: Linear Interpolation (*LI*), *Kalman* filter (models of constant velocity (*Kv*), constant acceleration (*Ka*) and constant jerk (*Kj*)) and $\alpha\beta/\alpha\beta\gamma$. In Figure 6, we can see the behavior of them for 1 dof. In this figure, we can see that the best filters are $\alpha\beta$ and *Kv* but using them is not possible to estimate acceleration or jerk movements. By other hand, if we use a *Kj* filter to estimate a constant velocity movement, it would not work properly. With the fuzzy filter, we can estimate a constant velocity or a constant jerk movement with a low adapting time.

The main idea is that for different conditions (velocity, acceleration and jerk) of the object's trajectory one filter works better than the others, in other words, for specific values of velocity and acceleration we must apply an specific filter or filters and not others depending of dispersion values for each case.

We have adjusted initial values empirically for the filter. Once we have these values, an optimization algorithm (trust region algorithm, see [30] and [31]) is executed to find the local minimum closest to empirical values selected. This optimization technique is applied off-line and before the prediction procedure during several experiments in which the characteristics were always inside the image plane.

Once the optimization algorithm is finished, characteristics can go out to the image and the filter will predict the trajectory properly.

The *Sugeno* type rules R_i [29][32][33] can be seen below:

- R_1 : IF $i \geq 5$ AND acceleration IS high AND acceleration > 0 AND jerk IS low THEN FuzzyFilter = $0.22 \cdot LI + 0.23 \cdot Kv + 0.26 \cdot Ka + 0.29 \cdot Kj$.
- R_2 : IF $i \geq 5$ AND acceleration IS high AND acceleration < 0 AND jerk IS low THEN FuzzyFilter = $0.26 \cdot LI + 0.74 \cdot Kv$.
- R_3 : IF $i \geq 5$ AND $j < 4$ AND acceleration IS low AND jerk IS low THEN FuzzyFilter = $0.33 \cdot LI + 0.67 \cdot Kv$.
- R_4 : IF $i \geq 5$ AND $j \geq 4$ AND acceleration IS low AND jerk IS low THEN FuzzyFilter = $0.21 \cdot LI + 0.56 \cdot \alpha\beta\gamma + 0.23 \cdot Kv$.
- R_5 : IF $i < 5$ THEN FuzzyFilter = $0.29 \cdot LI + 0.62 \cdot \alpha\beta\gamma + 0.09 \cdot Kv$.
- R_6 : IF $i \geq 5$ AND velocity IS low AND jerk IS low THEN FuzzyFilter = $0.18 \cdot LI + 0.55 \cdot \alpha\beta\gamma + 0.27 \cdot Kv$.

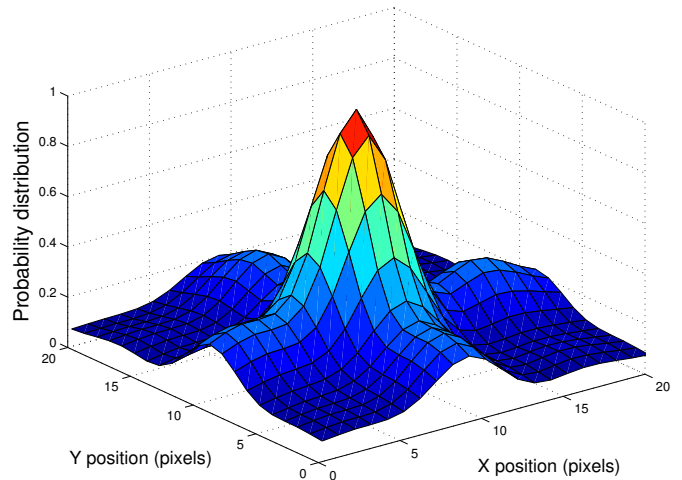


Fig. 7. Probability function of fuzzy filter

R_7 : IF jerk IS high THEN FuzzyFilter = *Kj*.

The membership input functions are presented in Figure 5 and parameters are defined as: $\begin{cases} \text{velocity,} & a=1 \ c=2; \\ \text{acceleration,} & a=3 \ c=4; \end{cases}$ Once these rules are established, we have the new fuzzy filter, see Figure 4.

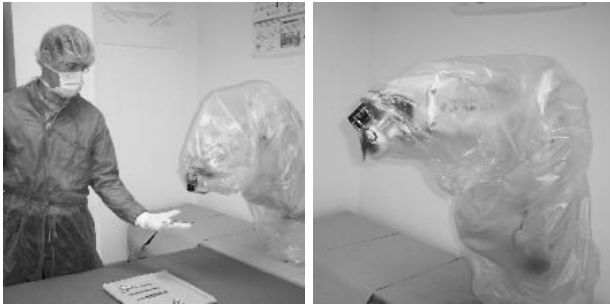
In Figure 7, we can see the probability function of the new filter. This function is similar to a gaussian function or like a Mexican-Hat wavelet in 3D. This probability function is the output of a function that uses as input the ten last points of one characteristic and returns the next position (Figure 7 take into account noise in input points introduced by the camera and feature recognition). z axis is the probability, and x, y are the predicted position.

4. EXPERIMENTAL RESULTS

Experimental results has been carried out using a 6 axis industrial manipulator (Fanuc LR Mate 200iB). The experimental setup used in this work also includes one camera (uEye) rigidly mounted in robot end effector, one electromagnetic device as robot gripper, an ELF force measurement system, some surgical surgical instruments and a computer with vision control system and other computer with the robot control system. An RPC link between the robot controller and the computer with the vision control system for synchronization tasks and data interchange has been implemented. The whole experimental setup can be seen in Figure 8.

In this experiment, the interaction matrix is assumed constant and determined during off-line step using the desired value of the visual features and an approximation of the points depth at the reference camera pose. The goal of the control is to retrieve the surgical instrument from the surgeon's hand by visual servoing techniques (Figure 8).

One of the main problems of visual servoing is the lose of some image features during the control process (produced by an out-coming of one or more image features). When this problem appears, several solutions have been tested: extract these features from s, weighted image features or



(a) Robotic system retrieving a surgical instrument
 (b) Robot with the surgical instrument retrieved

Fig. 8. Experimental Setup: robotic system proposed retrieving surgical instruments from the surgeon's hand by visual servoing techniques

simply stop the visual servoing control [19, 20, 6, 28]. The system is unstable when the extract of image features is used [19, 20]. When the weighted image features approach is used, the system is unstable because of most of the features is inside the Zone 2 (weights are equal to zero).

Using the 2D visual servoing approach in the extended image plane, the system is stable although one or more features leave the image plane (Figure 9). In Figure 9, the rectangle with dashed-line shows the control law when the prediction algorithm is used to compute the position of image features.

5. CONCLUSIONS AND FUTURE WORKS

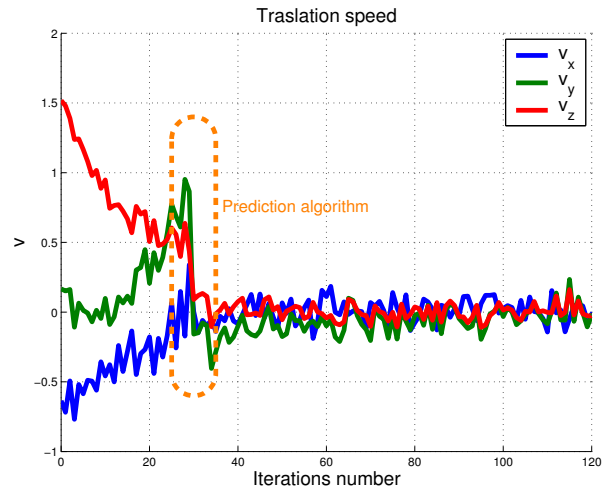
In this paper, the visibility problems in visual servoing when a robotic scrub nurse is retrieving the surgical instruments from the surgeon's hand are presented and a review of the different scientific works which deal this problem are recalled. After that, our solution to this problem based on the extended image plane is presented and compared with other solutions proposed in the literature. To estimate the image features in the extended image plane, a prediction filter was developed and its estimation error is computed. With the experimental results, it has been shown that the visual servoing in the extended image plane is continuous and locally stable in a neighborhood of the equilibrium point.

REFERENCES

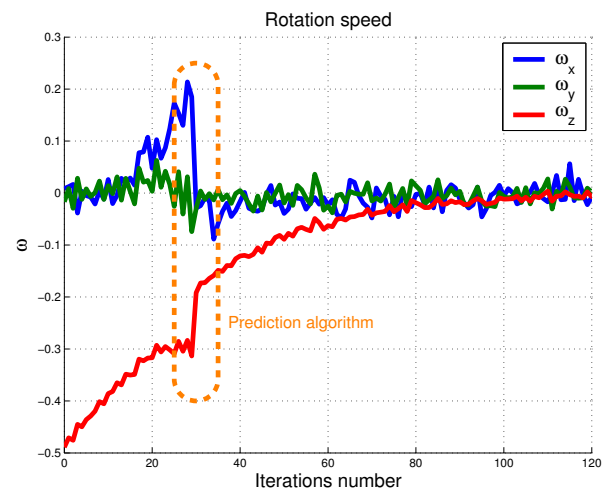
[1] M. R. Treat, S. E. Amory, P. E. Downey and D. A. Taliaferro, "Initial clinical experience with a partly autonomous robotic surgical instrument server", *Surgical Endoscopy*, ISSN: 0930-2794, 20(8):1310-1314, August, 2006

[2] C. Pérez, O. Reinoso, N. García, J.M. Sabater and J.M. Azorín. "Improvement of the visual servoing task with a new trajectory predictor. The Fuzzy Kalman Filter". International Conference on Informatics in Control, Automation and Robotics (ICINCO 2007). Angers (France). 9-12 May, 2007

[3] C. Pérez, N. García, J.M. Sabater, J.M. Azorín and O. Reinoso. "Object Trajectory Prediction. Application



(a) Translational velocity



(b) Rotational velocity

Fig. 9. Experimental results: visual servoing using the extended image plane approach

to Visual Servoing". European Control Conference (ECC 2007). Kos (Greece). 2-5 July, 2007

[4] C. Samson, M. Le Borgne, and B. Espiau. *Robot Control: the Task Function Approach*, volume 22 of *Oxford Engineering Science Series*. Clarendon Press, Oxford, UK, 1991.

[5] P. Rives B. Espiau, F. Chaumette. A new approach to visual servoing in robotics. *IEEE Trans. Robotics and Automation*, 8(3):313-326, June 1992.

[6] S. A. Hutchinson, G. D. Hager, and P. I. Corke. A tutorial on visual servo control. *IEEE Trans. Robotics and Automation*, 12(5):651-670, 1996.

[7] D. Kragic. Modeling, specification and robustness issues for robotic manipulation tasks. *International Journal of Advanced Robotic Systems*, 1(2):75-86, June 2004.

[8] D. Kragic and H. Christensen. Robust visual servoing. *International Journal of Robotic Research*, 10-

- 11(22):923–939, Oct-Nov 2003.
- [9] V. Kyrki, D. Kragic, H. Christensen. Measurement Errors in Visual Servoing Robotics and Autonomous Systems, Volume 54, Issue 10, pp 815-827, September 2006
- [10] E. Marchand, A.I. Comport, and F. Chaumette. Improvements in robust 2d visual servoing. In *IEEE Int. Conf. on Robotics and Automation, ICRA'04*, volume 1, pages 745–750, New Orleans, LA, April 2004.
- [11] A.I. Comport, M. Pressigout, E. Marchand, and F. Chaumette. A visual servoing control law that is robust to image outliers. In *IEEE Int. Conf. on Intelligent Robots and Systems, IROS'03*, volume 1, pages 492–497, Las Vegas, Nevada, October 2003.
- [12] P.I. Corke and S.A. Hutchinson. A new partitioned approach to image-based visual servo control. *IEEE Trans. on Robotics and Automation*, 17(4):507–515, August 2001.
- [13] Y. Mezouar and F. Chaumette. Path planning for robust image-based control. *IEEE Trans. on Robotics and Automation*, 18(4):534–549, August 2002.
- [14] Y. Mezouar and F. Chaumette. Optimal camera trajectory with image-based control. *Int. Journal of Robotics Research*, 22(10):781–804, October 2003.
- [15] G. Chesi, K. Hashimoto, D. Prattichizzo, and A. Vicino. Keeping features in the camera field of view: a visual servoing strategy. In *15th Int. Symp. on Mathematical Theory of Networks and Systems*, Notre-Dame, Indiana, August 2002.
- [16] G. Chesi, K. Hashimoto, D. Prattichizzo, and A. Vicino. Keeping features in the field of view in eye-in-hand visual servoing: a switching approach. *IEEE Trans. Robotics*, 20(5):908–913, 2004.
- [17] S. Benhimane and E. Malis. Vision-based control with respect to planar and non-planar objects using a zooming camera. In *IEEE International Conference on Advanced Robotics*, volume 2, pages 991–996, Coimbra, Portugal, July 2003.
- [18] F.Schramm and G.Morel. A calibration free analytical solution to image points path planning that ensures visibility. In *IEEE International Conference on Robotics and Automation*, volume 1, New Orleans, USA, 2004.
- [19] N. Garcia-Aracil and E. Malis. Preserving the continuity of visual servoing despite changing image features. In *In Proc. IEEE/RSJ International Conference on Intelligent Robots and Systems*, Sendai, Japan, October 2004.
- [20] N. Garcia-Aracil, E. Malis, O. Reinos, and R. Aracil. Parameters selection and stability analysis of invariant visual servoing with weighted features. In *In Proc. IEEE/RSJ International Conference on Robotics and Automation*, Barcelona, Spain, April 2005.
- [21] N. R. Gans and S. Hutchinson. An experimental study of hybrid switched system approaches to visual servoing. In *IEEE International Conference on Robotics and Automation*, volume 1, pages 3061–3068, Taipei, Taiwan, September 2003.
- [22] E. Malis and F. Chaumette. Theoretical improvements in the stability analysis of a new class of model-free visual servoing methods. *IEEE Transaction on Robotics and Automation*, 18(2):176–186, April 2002.
- [23] G. Morel, T. Liebezeit, J. Szewczyk, S. Boudet, , and J. Pot. Explicit incorporation of 2d constraints in vision based control of robot manipulators. In *Int.Symposium on Experimental Robotics*, volume 1, Sidney, Australia, 1999.
- [24] H. Zhang and J. P. Ostrowski. Visual motion planning for mobile robots. *IEEE Trans. Robotics and Automation*, 18(2):199–208, 2002.
- [25] N. Cowan, J. Weingarten, and D. Koditschek. Visual servoing via navigation functions. *IEEE Trans. on Robotics and Automation*, 18(4):521–533, 2002.
- [26] E. Malis. Visual servoing invariant to changes in camera intrinsic parameters. *IEEE Transaction on Robotics and Automation*, 20(1):72–81, February 2004.
- [27] N. Garcia-Aracil, E. Malis, R. Aracil and C. Perez. Continuous Visual Servoing despite the changes of visibility in image features. *IEEE Transaction on Robotics*, 21(6):1214–1220, December 2005.
- [28] F. Chaumette. Potential problems of stability and convergence in image-based and position-based visual servoing. In D. Kriegman, G. Hager, and A. Morse, editors, *The confluence of vision and control*, volume 237 of *LNCIS Series*, pages 66–78. Springer Verlag, 1998.
- [29] Sugeno, M., "Industrial applications of fuzzy control", Elsevier Science Publications Company, 1985.
- [30] Frank Vanden Berghen, "CONDOR: a constrained, non-linear, derivative-free parallel optimizer for continuous, high computing load, noisy objective functions", Ph. D. in the University of Brussels (ULB - Universit Libre de Bruxelles), Belgium. 2004.
- [31] M.J.D. Powell, "UOBYQA: Unconstrained Optimization BY Quadratic Optimization", DAMTP 2000/NA14. Math. Program. 92B, 555582.
- [32] Wang, Li-Xin, "Course in Fuzzy Systems and Control Theory", Imprint: Pearson US Imports & PHIPES. Publisher: Pearson Higher Education. Date Published: 4/06/1997
- [33] Wang, Li-Xin, "Course In Fuzzy Systems and Control, A", ISBN: 0-13-540882-2. Publisher: Prentice Hall Copyright: 1997